13

PARAFAC Analysis for Temperature-Dependent NMR Spectra of Poly(Lactic Acid) Nanocomposite

Hideyuki Shinzawa[1], Masakazu Nishida[1], Toshiyuki Tanaka[2], Kenzi Suzuki[3] and Wataru Kanematsu[1]
[1]*Research Institute of Instrumentation Frontier, Advanced Industrial Science and Technology (AIST)*
[2]*Mikawa Textile Research Center, Aichi Industrial Technology Institute (AITEC)*
[3]*Department of Chemical Engineering, Graduate School of Engineering, Nagoya University*
Japan

1. Introduction

This chapter provides a tutorial on the fundamental concept of Parallel factor (PARAFAC) analysis and a practical example of its application. PARAFAC, which attains clarity and simplicity in sorting out convoluted information of highly complex chemical systems, is a powerful and versatile tool for the detailed analysis of multi-way data, which is a dataset represented as a multidimensional array. Its intriguing idea to condense the essence of the information present in the multi-way data into a very compact matrix representation referred to as scores and loadings has gained considerable popularity among scientists in many different areas of research activities.

The basic idea of PARAFAC is so flexible and general that its application is not limited to a particular field of spectroscopy confined to a specific electromagnetic probe. Examples of the application include fluorescence (Christensen *et al.,* 2005; Rinnan *et al.,* 2005), IR (Wu *et al.,* 2003), NMR (Bro *et al.,* 2010), UV (Ebrahimi et al., 2008; Van Benthem et al., 2011) and mass spectroscopy (Amigo *et al.,* 2008). The first part of this chapter covers the theoretical background of trilinear decomposition of three-way data by PARAFAC with comparison to bilinear decomposition of two-way data by Principal component analysis (PCA).

In the second part of this chapter, an illustrative example of PARAFAC analysis for three-way data obtained in an actual laboratory experiment is presented to show how PARAFAC trilinear model can be constructed and analyzed to derive in-depth understanding of the system from the data. Thermal deformation of several types of poly lactic acid (PLA) nanocomposites undergoing grass-to-rubber transition is probed by cross-polarization magic-angle (CP-MAS) NMR spectroscopy. Namely, sets of temperature-dependent NMR spectra are measured under varying clay content in the PLA nanocomposite samples. While temperature strongly affects molecular dynamics of PLA, the clay content in the samples also influences the molecular mobility. Thus, NMR spectra in this study become a three-way

dataset described as a function of both temperature and clay content. Details of the effects of the temperature and clay content on the physical state of nanocomposite are elucidated by using PARAFAC trilinear model.

2. PARAFAC

2.1 Multi-way data

So, what does a multi-way data look like? It is insightful first to note the data structures of two-way and three-way data. Schematic descriptions of two-way and three-way data based on external perturbation(s) are shown in Fig. 1. In a general spectroscopic measurement, external perturbations are applied to the system of interest to induce the response to the stimuli. Characteristic response of the system is presented in the form of spectrum. For example, when the thermal behaviour of a sample is studied by a spectroscopic method, such as IR, Raman and NMR, the sample is heated up to undergo thermal deformation and its molecular level variation induced by the stimulus is captured at each spectral variable, e.g. wavenumber. The spectral dataset thus obtained will be represented as a two-way array with the *(i,j)*th element denoting the spectral intensity value at the *i*th temperature and the *j*th wavenumber.

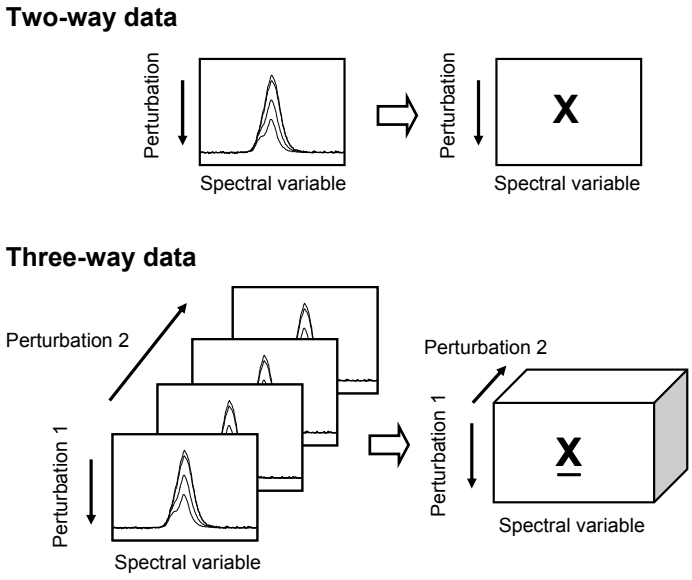

Fig. 1. Schematic illustration of two-way and three-way data.

Now, let us consider another experiment with one more perturbation. As described above, stimulation of a single sample ends up with two-way data array. But what if we still have some more samples, whose properties (e.g. concentration) are different? We will repeat a similar experiment for every single sample. This generates multiple two-way data. Thus, the entire dataset eventually becomes a stuck of the multiple two-way data like a cube, which contains two dimensions concerning applied two perturbations. Such spectral dataset is

described as a three-way array with the *(i,j,k)*th element denoting the spectral intensity value at the *i*th concentration, the *j*th temperature, and the *k*th wavenumber. For example, the samples will show the variation of their molecular structure depending on the temperature. This may be also influenced by the change in the concentration. Thus the spectral intensities of the samples are potentially influenced by the temperature as well as concentration.

2.2 PARAFAC model

It is possible to condense the essence of the information present in multi-way data into a very compact matrix representation referred to as scores and loadings. The basic hypothesis of factor analysis techniques is that the improved proxy of the original data matrix can be reconstructed from only a limited number of significant factors. Thus, while the score and loading matrices contain only a small number of factors, it effectively carries all the necessary information about spectral features and, eventually, it becomes possible to sorting out the convoluted information content of highly complex chemical systems. The detailed analysis of such matrices potentially brings useful insight into building a mechanistic model for understanding complex phenomena studied by spectroscopic method.

Principal component analysis (PCA) is mathematical decomposition of two-way data in terms of the orthogonal set of dominant factors, i.e., eigenvectors (Smilde *et al.,* 2004; Shinzawa *et al.,* 2010). Two-way data decomposition by PCA results in yielding two matrices called scores and loadings which complementarily represent the entire features broadly distributed in the two-way data as follows,

$$\mathbf{X} = \mathbf{T}\mathbf{P}^{\mathbf{t}} + \mathbf{E}_{\mathbf{PCA}} \tag{1}$$

where **T** and **P** are PCA score and loading matrices consisting of *r* vectors, respectively. The rank *r* corresponds to the number of principal components representing the significant portion of the information contained within the data matrix **X**. The selection of *r* is somewhat arbitrary. It is usually set to be a number, as small as possible but sufficiently large enough such that there are no obvious spectral features found in the residual matrix $\mathbf{E}_{\mathbf{PCA}}$. The residual matrix $\mathbf{E}_{\mathbf{PCA}}$ is the portion of the original data, which is not accounted for by the first *r* principal components used for the data representation. The two matrices **T** and **P** complementally represent the entire features broadly distributed in **X**. Namely, **T** holds abstract information concerning the relationship among the samples and **P** contains summary of variable, e.g. wavenumber which provides chemically or physically meaningful interpretation to the pattern observed in **T**. For example, PCA of the two-way data based on temperature-dependent spectra provides **T** describing similar or dissimilar thermal behaviour of the sample during the perturbation period and corresponding **P** represent information on key molecular structure associated with such similar or dissimilar thermal behaviour of the sample.

For even more data, PARAFAC is used to decompose a multi-way data and Fig. 2 illustrates graphical representation of PARAFAC operation to decompose a three-way data into score and loading vectors. PARAFAC is utilized to decompose the multi-way data into a linear combination of score and loading matrices (Smilde *et al.,* 2004; Bro, 2004). The information on behavior induced by the perturbations is effectively described by score vectors and corresponding loading vectors provide chemically or physically meaningful interpretation

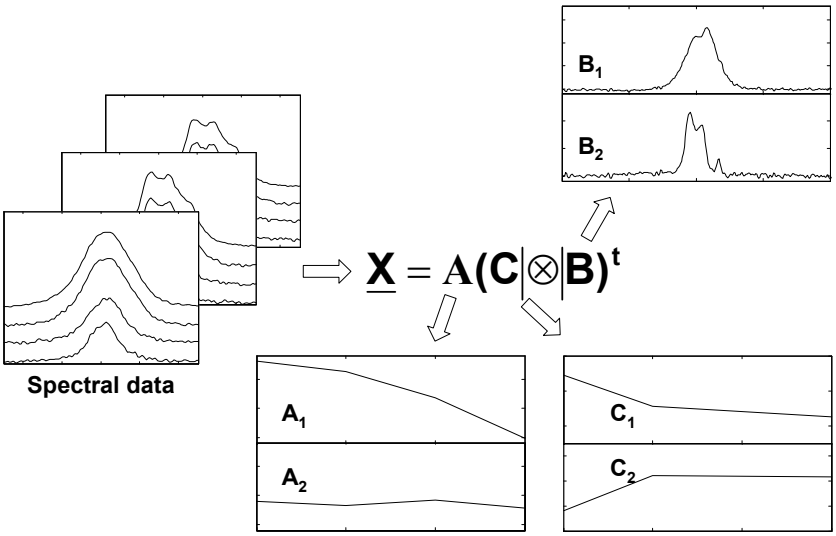

Fig. 2. Schematic illustration of PARAFAC trilinear model.

to the patterns observed in the scores of the PARAFAC trilinear model. Namely, by using PARAFAC operation, $I \times J \times K$ array matrix $\underline{\mathbf{X}}$ can be expressed in terms of a product of score and loading matrices, **A**, **B**, and **C**, and a residual matrix **E** as follows

$$\mathbf{X}^{(I\times JK)} = \mathbf{A}(\mathbf{C}\left|\otimes\right|\mathbf{B})^{\mathbf{t}} + \mathbf{E}^{(I\times JK)} \tag{2}$$

where ($I \times JK$) refers to the way that the multi-way array is unfolded. The notation $\left|\otimes\right|$ means Khatri-Rao product which operate Kronecker product $\left|\otimes\right|$ on partitioned matrices defined as

$$\mathbf{C}\left|\otimes\right|\mathbf{B} = [\mathbf{c_1} \otimes \mathbf{b_1} \quad \mathbf{c_2} \otimes \mathbf{b_2} \quad \cdots \quad \mathbf{c}_F \otimes \mathbf{b}_F] \tag{3}$$

In PARAFAC analysis, the set of matrices **A**, **B** and **C** are usually obtained by iteratively solving alternating least-squares (ALS) problems $\min_{\mathbf{A},\mathbf{B},\mathbf{C}} \left\| \mathbf{X}^{(I\times JK)} - \mathbf{A}(\mathbf{C}\left|\otimes\right|\mathbf{B})^{\mathbf{t}} \right\|$ over **A** for fixed **B** and **C,** as well as the minimization over **B** or **C** in the similar matrix operation manner under appropriate model constraints, such as the non-negativity of concentration and spectral intensity (Bro & de Jong, 1997; Bro & Sidiropoulos, 1998). General procedure of PARAFAC becomes as follows,

Initialize **B** and **C** to obtain **Z** as

$$\mathbf{Z} = \mathbf{C} \otimes \mathbf{B} \tag{4}$$

A is given by

$$\mathbf{A} = \mathbf{X}^{(I\times JK)}\mathbf{Z}(\mathbf{Z}^{t}\mathbf{Z})^{+} \tag{5}$$

where the superscript + means the Moore-Penrose inverse. Then update **Z** as

$$\mathbf{Z} = \mathbf{C} \otimes \mathbf{A} \tag{6}$$

B is obtained as

$$\mathbf{B} = \mathbf{X}^{(J\times IK)}\mathbf{Z}(\mathbf{Z}^{t}\mathbf{Z})^{+} \tag{7}$$

Update **Z** as

$$\mathbf{Z} = \mathbf{B} \otimes \mathbf{A} \tag{8}$$

C is given by

$$\mathbf{C} = \mathbf{X}^{(K\times IJ)}\mathbf{Z}(\mathbf{Z}^{t}\mathbf{Z})^{+} \tag{9}$$

If the residual between the original $\underline{\mathbf{X}}$ and reconstructed $\underline{\mathbf{X}}$ by Eq. 2 is greater than error criteria, one repeats Eqs. (4)-(9) until convergence.

The initial estimates for **B** and **C** is important to obtain sufficient minimization of the error criteria (Shinzawa *et al.,* 2007, 2008a & 2008b). Although ALS algorithm usually offers an eventual convergence to the optimal solution with a sufficiently large number of iterations, it sometimes reaches the suboptimal local minimum (Jiang *et al.,* 2003 & 2004). Unfortunately, such local convergence does not usually offer a global minimum, but it may just be stuck in a local minimum, producing insufficient solution. The major cause of the suboptimal local convergence may be a poor initial estimation. One possible solution for this problem is to select proper initial estimate which is less sensitive to the presence of a local minimum, e.g. via signaler value decomposition (Bro & de Jong, 1997; Bro & Sidiropoulos, 1998; Wang *et al.,* 2006; Awa *et al.,* 2008).

3. Example

3.1 PLA nanocomposite

A pertinent example for PARAFAC analysis based on NMR spectra of PLA nanocomposites is provided here to show how certain useful information can be effectively extracted from an actual laboratory experiment.

Fig. 3 shows the molecular structure of PLA. PLA polymer is made up of many long chains consisting of the repeat unit shown in the figure. PLA is derived from renewable resources, such as corn starch via fermentation and it is biodegradable under the right conditions, such as the presence of oxygen (Tsuji *et al.,* 2010). Thus, PLA is a possible candidate of a new class of renewable polymers as a substitute for the petrochemical polymers. However, the physical properties of PLA are inadequate for the replacement of conventional commodity plastics in many applications.

Nanocomposite is a technique to improve the physical strength, thermal resistance and gas barrier by the dispersion of nanoclay into the polymer (Katti *et al.,* 2006). The improvement

of such polymer properties by using nanocomposite is one of the primary areas of interest due to its potential applications. The polymer nanocomposites are generally formed by the addition of a small amount of nanoclay dispersion.

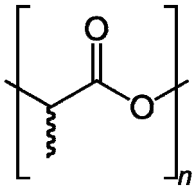

Fig. 3. Molecular structure of PLA.

Fig. 4 shows a schematic illustration of polymer nanocomposite. A typical form of the nanocomposite is intercalated nanocomposite, in which the unit cells of clay structure are expanded by the insertion of polymer into the interlayer spacing, while the periodicity of clay crystal structure is maintained. Most commonly, montmorillonite (MMT) is used as clay due to its highly expansive characteristic (Suguna Lakshmi *et al.*, 2008; Cervantes-Uc *et al.*, 2009). The MMT unit cell is composed of aluminum octahedra sandwiched between two silica tetrahedra with the unit cell dimension of about 1 nm in thickness. For facilitating better miscibility of hydrophobic polymer with the clay and increasing the spacing of the interlayer clay gallery, it is often treated with organic modifiers which are generally long carbon chain compounds with alkylammonium or alkylphosphonium cations.

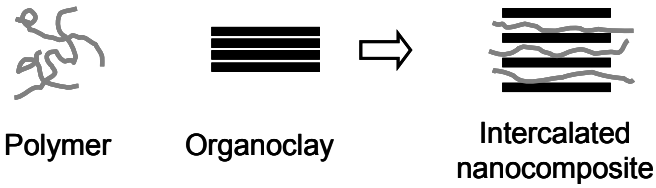

Fig. 4. Schematic illustration of polymer nanocomposite.

PLA nanocomposite samples used in this study were prepared with PLA (Teramac®, Unitika) and organically modified clay (S-BEN W®, Hojun). The samples were put into a Labo-plastomill consisting of a 30C150 kneader and an R100 mixer (Toyo Seiki Seisaku-sho, Ltd., Tokyo) to melt-blend at 190 °C and 50 rpm for about 10 minutes. Pellets thus obtained were pressed into 0.2 mm thick sheet sandwiched between two thick Teflon® films by a hot press at 190 °C.

Fig. 5 represents the effect of nanocomposite on PLA probed by Thermomechanical analysis (TMA). TMA is a technique to monitor the physical deformation of object under a constant load, while varying the temperature. For example, in this case, the elongation of the PLA nanocomposite samples (clay content = 0, 5 and 15 wt%) were measured by imposing a 9.8 mN load, while varying the temperature from 35 to 140 °C at a rate of 10 °C per a minute. The elongation of the samples starts when the temperature reaches glass transition temperature (T_g) of PLA, i.e. approximately 60 °C (Zhang et al., 2010). Then it gradually

increases with the increase of temperature and it finally reached constant levels at the close of the observation period, indicating that the observed plastic deformation is closely related to glass-to-rubber transition of the amorphous component of PLA. It is also noted that the samples results in the different levels of elongation depending on the clay content. For example, the neat PLA sample shows 14.4 % of elongation. In contrast, the PLA-nanocomposite including 15 wt % of clay ends up with 9.1 % of elongation. The leveling off of the elongation indicates the formation of a network structure due to the presence of physical crosslinks created by the crystalline domain.

Although such observation effectively detects the macroscopic changes in the mechanical properties caused by the presence of clay particles, additional fundamental molecular level understanding of the reinforcement mechanism is also desired. Spectroscopic method should become an important tool to probe the phenomena at the molecular level.

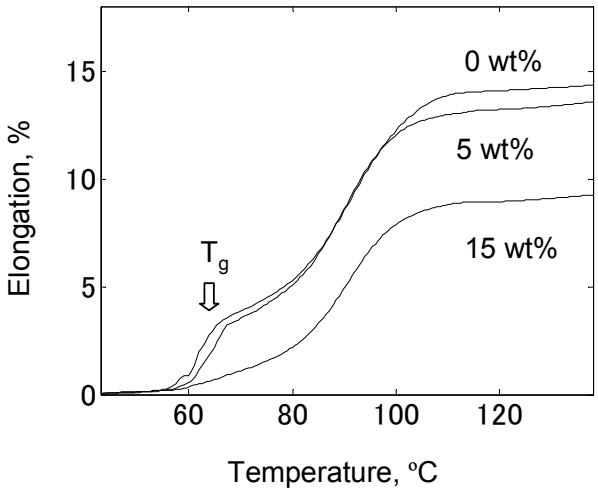

Fig. 5. Physical property of PLA samples proved by TMA.

3.2 PALAFAC analysis of NMR spectra of PLA nomocomposites

The temperature-dependent NMR spectra of the PLA samples collected under the varying temperature from 20 to 80 °C are shown in Fig. 6. Cross polarization-magic angle spinning (CP-MAS) NMR experiments were carried out on a Varian 400 NMR system spectrometer operated at 100.56 MHz for ^{13}C resonance with a cross polarization contact time of 2 ms (Fawcett, 1996). A zirconium oxide rotor of 4 mm diameter was used to acquire the NMR spectra at a spinning rate of 15 kHz. Each sample was packed into a 4 mm cylinder-type MAS rotor. A set of temperature-dependent NMR spectra were obtained under varying ambient temperature from 20 to 80 °C at every 20 °C step. The heating rate was approximately 10 °C per an hour.

Samples of semicrystalline polymers prepared from their melt possess complex supermolecular structure consisting of crystalline lamellae embedded in an amorphous

matrix (Wunderlich, 1980). PLA essentially undergoes highly convoluted transition process, when temperature and its constitution are altered. These transitions include the melting of ordered molecular segments, as well as the grass-to-rubber transition and other relaxation of process of the amorphous component (Zhang et al., 2005; Meaurio *et al.*, 2006).

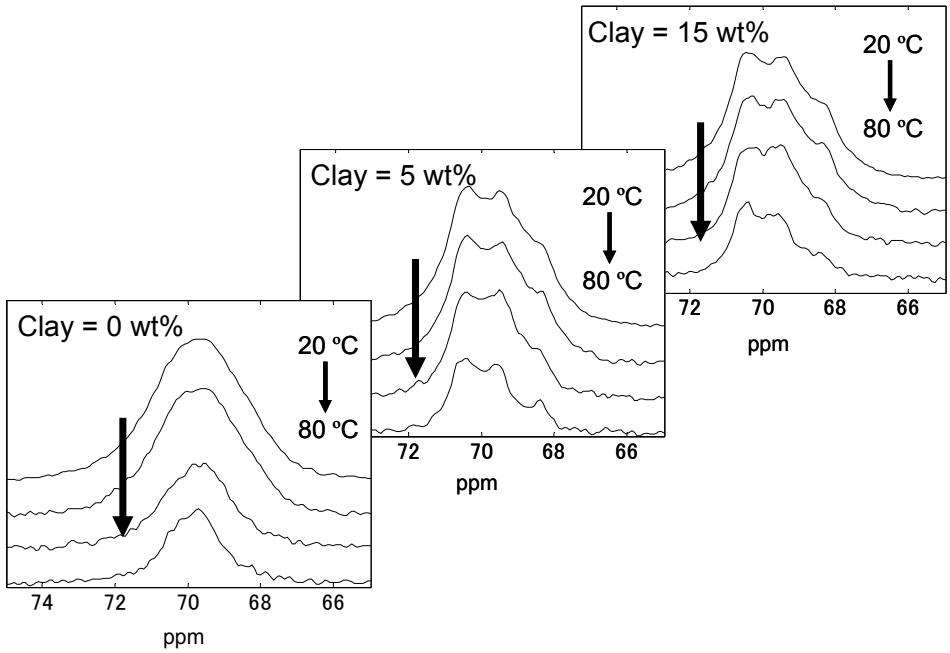

Fig. 6. Temperature-dependent CP-MAS NMR spectra of neat PLA and PLA nanocomposite samples.

The CP-MAS technique is ideal for the observation of ^{13}C spectra of solid samples. Since the local environment of a chemical group in solids are generally rigid, this leads to further considerations for crystallography or, more generally, molecular packing (Fawcett, 1996). The CPMAS NMR study of semicrystalline PLA samples is often complicated by the presence of overlapped contributions from coexisting crystalline and amorphous. For example, the unimodal peak observed around 69.5 ppm is assignable to CH structure which represents mobility of the main chain of the PLA (Tsuji *et al.*, 2010; Kister *et al.*, 1998). It is noted that the peak intensity gradually decreases with the increase of the temperature. This may be explained as the decrease in the cross polarization efficiency by the change in the molecular dynamics during the heating. Thus, the variation of the spectral intensity here reflects the structural alternation of PLA induced by the temperature.

More importantly, careful comparison of the samples reveals that the main feature of the NMR spectra of the three samples looks somewhat different. For example, the temperature-dependent NMR spectra of the PLA nanocomposite including 15 wt% clay provides specific three peaks at 70.5, 69.5 and 68.4, indicating the presence of the crystalline structure in the sample (Tsuji *et al.*, 2010; Kister *et al.*, 1998). When the sample has no clay in the system,

these crystalline peaks are disappeared and compensated by the development of seemingly unimodal peak probably assigned to the amorphous of PLA (Tsuji *et al.,* 2010; Kister *et al.,* 1998). This indicates that the presence of the clay substantially influences supermolecular structure of the PLA. Consequently, it is very likely that the change in the spectral feature of the three-way data is closely related to temperature and clay content of the system. Thus, in turn, the fully detailed analysis of the data provides an interesting opportunity to probe the nature of the PLA nanocomposite by elucidating the variation of the NMR spectral intensity induced by the each perturbation with PARAFAC trilinear decomposition.

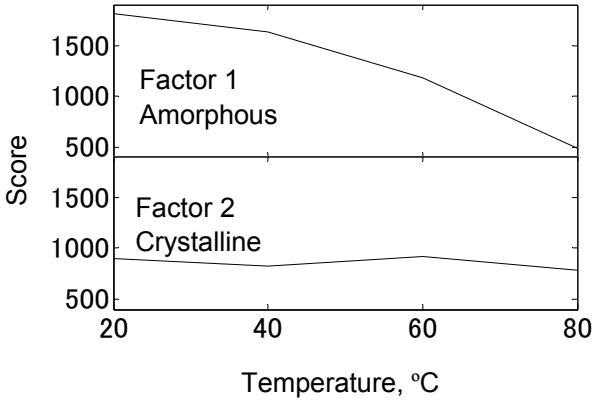

Fig. 7. Score vectors in score matrix **A** representing thermal behaviours of amorphous and crystalline components in PLA samples.

Fig. 7, 8 and 9 show results obtained from **A**, **B** and **C** matrices derived from PARAFAC analysis of the three-way NMR spectral data collected under varying temperature and clay content, respectively. Two major factors are indicated here, reflecting the fact that there are two species present in the system. One of the important benefits derived from PARAFAC decomposition of the multi-way data is the ability to rationally clarify the effect of the applied perturbations. For example, the matrix **A** represents abstract information on the temperature-induced behavior of the PLA under the influence of the clay content. In contrast, the matrix **C** holds essential information on the spectral intensity variation induced by the addition of the clay under the influence of the temperature. The matrix **B** contains loading vectors which provides chemical or physical interpretation to the patterns observed in the score matrices **A** and **C**.

It is noted that the loading vector of the first component of the matrix **B** (Fig. 8) resembles the spectral feature of the amorphous component of PLA. The loading vector of the second component of the matrix **B** shows characteristic three peaks assignable to crystalline component of the PLA. Thus it is most likely that the second factor represents thermal behaviours of the crystalline components in PLA samples.

Once the assignments for the loading vectors are established, it becomes possible to provide chemically meaningful interpretation to the score matrices **A** and **C** representing the dynamic behaviour of the components induced by the perturbations. For example, the score

vector of the first factor in the matrix **A** represents the temperature-induced behaviour of the amorphous component of the PLA. On the other hand the score vector of the second factor means that of the crystalline component of the PLA. It is noted the score vector of the amorphous components exhibits obvious decrease with the temperature and such decrease becomes significant when the temperature exceeds its T_g. In contrast, the change in the score value of the crystalline component is small, indicating no major variation during the heating process.

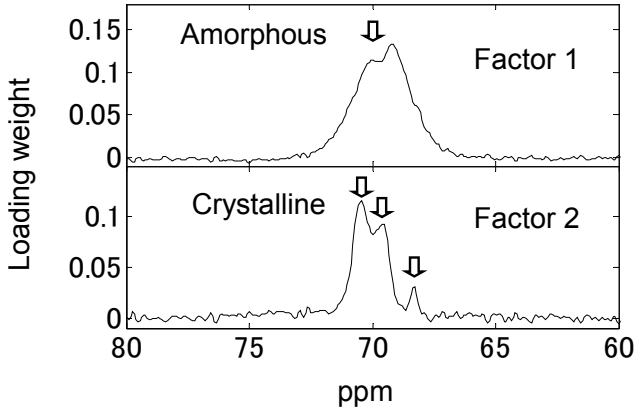

Fig. 8. Loading vectors in score matrix **B** representing thermal behaviours of amorphous and crystalline components in PLA samples.

The predominant variation of the amorphous component in the temperature region is explained as its glass-to-rubber transition. The change induced in the temperature region is associated with the Micro-Brownian motion of the PLA polymer segment. At a low temperature the amorphous regions of a polymer are in the glassy state. In this state the molecules are frozen on place. They may be able to vibrate slightly, but do not have any segmental motion. When the polymer is heated up to reach its T_g, the molecules can start to wiggle around to become rubbery state. Such segmental motion predominantly occurs in amorphous region of PLA while such motion is strongly restricted in systematically folded crystalline lamellae structure. Thus, it is very likely the observed change of the amorphous is related to glass-to-rubber transition of the amorphous component.

Now it is important to point out again that the predominant elongation in the TMA occurred around T_g. This elongation behaviour agrees well with the thermal behaviour of the amorphous component observed in the score matrix **A**. It thus suggests the physical elongation of the samples is essentially associated with the glass-to-rubber transition mainly occurred in the amorphous region.

It also becomes possible to provide the detailed interpretation to the pattern observed in the matrix **C** representing the clay-induced behaviours of amorphous and crystalline components in the PLA samples. The gradual decrease of the score of the first factor can be explained as the decrease of the amorphous component and the change in the sore of the first factor corresponds to the increase in the crystalline component by the addition of the

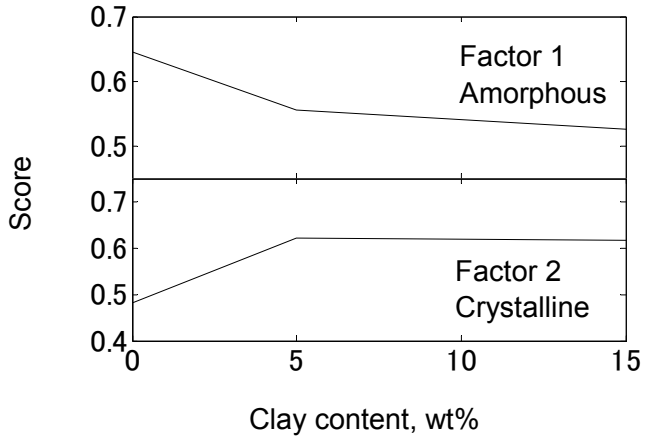

Fig. 9. Score vectors in score matrix **C** representing clay-induced behaviours of amorphous and crystalline components in PLA samples.

clay. It seems that the decrease in the amorphous is compensated by the development of the crystalline structure. In other words, the clay increases the frequency of the spontaneous nucleation of the PLA crystals.

PARAFAC trilinear model of the three-way NMR data of the PLA nanocomposites reveals that the crystalline and amorphous structures of the PLA nanocomposites undergo different transition under the heating. Namely, the change in the micro-Brownian motion of the polymer segments mainly occurs in the amorphous region. In addition, the different variations between the crystalline and amorphous component suggest the different effects of the presence of clay particles on them, i.e. nucleating effect of the clay. The decrease in the amorphous portion should result in the reduction of the structure undergoing the glass-to-rubber transition. Such variation of the crystallinity agrees well with the decreased elongation observed in the TMA. For example, in Fig. 5, the level of the elongation starting around T_g clearly decreases with the inclusion of the clay.

This hypothesis is also clearly supported with corresponding transmission electron microscope (TEM) images and differential scanning calorimetry (DSC) results of the PLA nanocomposite sample. Fig. 10 represents the TEM images of the PLA nanocomposite sample including 15 wt% clay. For example, in Fig. 10(a), one can see that the clay is broadly distributed over the PLA matrix. On the other hand, Fig. 10(b) reveals that some parts of the interlayer gallery is obviously extended, suggesting the insertion of the PLA polymer into the clay layers, namely intercalation.

DSC curves of the PLA samples, represented in Fig. 11, clearly show the presence of glass transition temperature around 60 °C. It is important to point out that this glass-to-rubber transition of amorphous component agrees well with the change in the elongation observed in the TMA. More importantly, the samples also provide obvious crystallization peak around 110 °C. The crystallization peak shows gradual increase by the inclusion of the clay content, suggesting quantitative increase in the amount of the crystalline structure. Thus, it

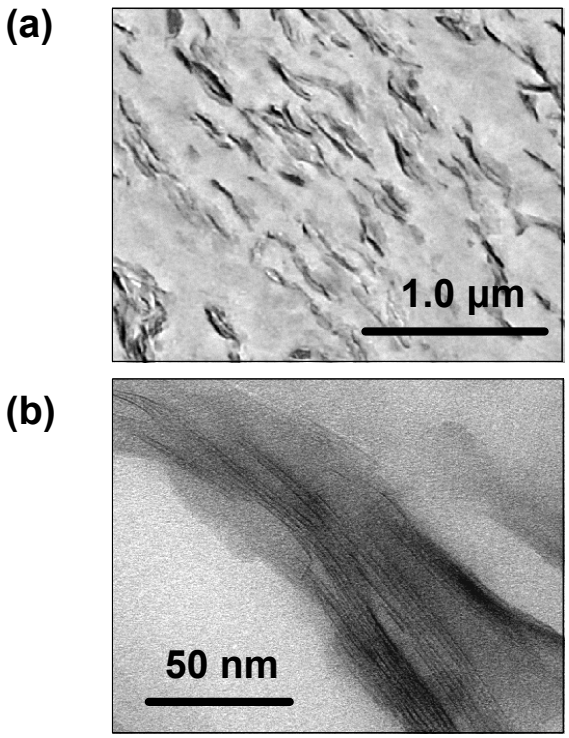

Fig. 10. TEM images of PLA nanocomposite sample.

is very likely that the clay works as the nucleating agent to increase the frequency of the spontaneous nucleation of the PLA crystals.

All the results put together, it provides overall picture of the system. When the clay is dispersed in the PLA matrix, the PLA polymer located at interlayer or around surface layer of the clay develops crystalline structure more frequently. The generation of the crystalline structure of PLA is compensated by the decrease of the amorphous content. This should decrease the structural portion substantially undergoing glass-to-rubber transition above T_g. Thus, in turn, it restricts the elongation of the samples during the heating process under a certain level of load. Consequently, it is demonstrated that PARAFAC analysis of the three-way data of the PLA nanocomposite samples effectively elucidates the mechanisms of the improvement of the mechanical property by the clay. By carrying out detailed band position shift analysis of the three way data of the temperature- and clay- dependent NMR spectra of the PLA samples, it becomes possible to extract chemically meaningful information concerning the variation of the crystalline structure closely associated with the nanocomposite system.

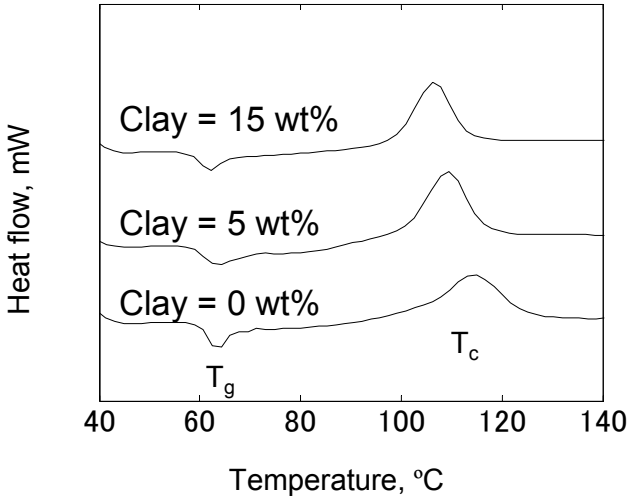

Fig. 11. DSC curves of neat PLA and PLA nanocomposite samples.

3. Conclusion

The basic background of PARAFAC and its practical example based on the temperature-dependent NMR spectra of the PLA nanocomposite samples are presented. The central concept of PARAFA decomposition of multi-way data lies in the fact that it can condense the essence of the information present in the multi-way data into a very compact matrix representation referred to as scores and loadings. Thus, while the score and loading matrices contain only a small number of factors, it effectively carries all the necessary information about spectral features and leads to sorting out the convoluted information content of highly complex chemical systems.

The effect of PLA nanocomposite is studied by the PARAFAC analysis of the temperature-dependent NMR spectra of several PLA nanocomposite samples including different clay contents. The PARAFAC analysis for the three-way data of the PLA nanocomposites revealed that the crystalline and amorphous structures of the PLA nanocomposites substantially undergo different transition under the heating. Namely, the change in the micro-Brownian motion of the polymer segments mainly occurs in the amorphous region when the PLA samples are heated up to their T_g. It also revealed that clay potentially works as nucleating effect of the clay. Namely, it increases the frequency of the spontaneous nucleation of the PLA crystals. Thus, in turn, the change in the population of the rigid crystalline and rubbery amorphous provides the improvement of the physical property. Consequently, it is possible to derive in-depth understanding of the PLA nanocomposites.

4. Acknowledgment

A part of this work was financially supported by NEDO "Technological Development of Ultra-hybrid Materials" Project.

5. References

Amigo, J. M., Skov, T., Coello, J., Maspoch, S. & Bro, R. (2008) Solving GC-MS problems with PARAFAC2. *TrAC Trends in Analytical Chemistry,* Vo. 27, No. 8, pp. 714-725

Awa, K., Okumura, T., Shinzawa, H., Otsuka, M. & Ozaki, Y. (2008). Self-modeling Curve Resolution (SMCR) Analysis of Near-infrared (NIR) Iimaging Data of Pharmaceutical Tablets. *Analytica Chimica Acta*, Vol. 619, No. 1, pp. 81-86

Bro, R. (2004). PARAFAC. Tutorial and applications. *Chemometrics and Intelligent Laboratory Systems*, Vol. 37, No. 2, pp. 149-171

Bro, R. & de Jong, S. (1997). A fast non-negativity constrained linear least squares algorithm for use in multi-way algorithms. *Journal of Chemometrics*, Vol. 11, No. 5, pp. 393-401

Bro, R. & Sidiropoulos, N. (1998). Least squares algorithms under unimodality and non-negativity constraints. *Journal of Chemometrics.* Vol. 12, No. 4, pp. 223–247

Bro, R., Viereck, N., Toft, M., Toft, H., Hansen, P. I. & Engelsen, S. B. (2010). Mathematical chromatography solves the cocktail party effect in mixtures using 2D spectra and PARAFAC. *TrAC Trends in Analytical Chemistry*, Vol. 29, No. 4, pp. 281-284

Cervantes-Uc, J. M., Espinosa, J. I. M., Cauich-Rodriguez, J. V., Avila-Ortega, A., Vazquez-Torres, H., Marcos-Fernandez. A. & San Roman, J. (2009). TGA/FTIR studies of segmented aliphatic polyurethanes and their nanocomposites prepared with commercial montmorillonites. *Polymer Degradation and Stability,* Vol. 94, No. 10, pp. 1666-1677

Christensen, J., Miquel Becker, B. & Frederiksen, C. S. (2005). Fluorescence spectroscopy and PARAFAC in the analysis of yogurt. *Chemometrics and Intelligent Laboratory Systems,* Vol. 75, No. 2, pp. 201-208

Ebrahimi, D., Kennedy, D. F., Messerle, B. A. & Hibbert, D. B. (2008). High throughput screening arrays of rhodium and iridium complexes as catalysts for intramolecular hydroamination using parallel factor analysis. *Analyst,* Vol. 133, No. 6, pp. 817-822

Fawcett, A. H. (1996). *Polymer Spectroscopy*, John Wiley & Sons, ISBN 0471960292, West Sussex, UK

Jiang, J.-H., Šašic, S., Yu, R.-Q. & Ozaki, Y. (2003). Resolution of two-way data from spectroscopic monitoring of reaction or process systems by parallel vector analysis (PVA) and window factor analysis (WFA): inspection of the effect of mass balance, methods and simulations. *Journal of Chemometrics*, Vol. 17, No. 3, pp. 186-197

Jiang, J.-H., Liang, Y. & Ozaki, Y. (2004). Principles and methodologies in self-modeling curve resolution. *Chemometrics and Intelligent Laboratory Systems*, Vol. 71, No. 1, pp. 1-12

Katti, K. S., Sikdar, D., Katti, D. R., Ghosh, P. & Verma. D. (2006). Molecular interactions in intercalated organically modified clay andclay–polycaprolactam nanocomposites: Experiments and modeling. *Polymer,* Vol. 47, No. 1, pp. 403-414

Kister, G., Cassanas, G. & Vert, M. (1998). Structure and morphology of solid lactide-glycolide copolymers from ^{13}C n.m.r., infra-red and Raman spectroscopy. *Polymer,* Vol. 39, No. 15, pp. 3335-3340

Meaurio, E., Zuza, E., López-Rodríguez. N. & Sarasua, J. R. (2006). Conformational Behavior of Poly(L-lactide) Studied by Infrared Spectroscopy. *Journal of Physical Chemistry B*, Vol. 110, No. 11 pp. 5790-5800

Rinnan, Å. & Andersen, C. M. (2005). Handling of first-order Rayleigh scatter in PARAFAC modelling of fluorescence excitation–emission data. *Chemometrics and Intelligent Laboratory Systems,* Vol. 76, No. 1, pp. 91-99

Shinzawa, H., Iwahashi, M., Noda, I. & Ozaki. Y. (2008a). Asynchronous Kernel Analysis for Binary Mixture Solutions of Ethanol and Carboxylic Acids. *Journal of Molecular Structure*, Vol. 883-884, No. 30, pp. 27-30

Shinzawa, H., Iwahashi, M., Noda, I. & Ozaki, Y. (2008b). A Convergence Criterion in Alternating Least Squares (ALS) by Global Phase Angle. *Journal of Molecular Structure*, Vol. 883-884, No. 30, pp. 73-78

Shinzawa, H., Jiang, J.-H., Iwahashi, M., Noda, I. & Ozaki, Y. (2007). Self-modeling Curve Resolution (SMCR) by Particle Swarm Optimization (PSO). *Analytica Chimica Acta*, Vol. 595, No. 1-2, pp. 275-281

Shinzawa, H., Awa, K., Kanematsu, W. & Ozaki, Y. (2010). Multivariate Data Analysis for Raman Spectroscopic Imaging. *Journal of Raman Spectroscopy,* Vol. 40, No. 12, pp. 1720-1725

Smilde, A., Bro, R. & Geladi, P. (November 2004). Multi-way Analysis: Applications in the Chemical Sciences. John Wiley & Sons, ISBN: 0471986911, West Sussex, UK

Suguna Lakshmi, M., Narmadha, B. & Reddy, B. S. R. (2008). Enhanced thermal stability and structural characteristics of different MMT-Clay/epoxy-nanocomposite materials. *Polymer Degradation and Stability,* Vol. 93, No. 1, pp 201-213

Tsuji, H., Kamo, S. & Horii, F. (2010). Solid-state ^{13}C NMR analyses of the structures of crystallized and quenched poly(lactide)s: Effects of crystallinity, water absorption, hydrolytic degradation, and tacticity. *Polymer,* Vol. 51, No. 10, pp. 2215-2220

Van Benthem, M. H., Lane, T. W., Davis, R. W., Lane, R. D. & Keenan, M. R., (2011). PARAFAC modeling of three-way hyperspectral images: Endogenous fluorophores as health biomarkers in aquatic species, *Chemometrics and Intelligent Laboratory Systems,* Vol. 106, No. 1, pp. 115-124

Wang, Z.-G., Jiang, J.-H., Ding, Y.-J., Wu, H.-L. & Yu, Ru-Qin., (2006). Trilinear evolving factor analysis for the resolution of three-way multi-component chromatograms. *Analytica Chimica Acta*, Vol. 558, No. 1-2, pp. 137-143

Wu, Y., Yuan, B., Zhao, J.-G. & Ozaki, Y. (2003). Hybrid Two-Dimensional Correlation and Parallel Factor Studies on the Switching Dynamics of a Surface-stabilized Ferroelectric Liquid Crystal. *Journal of Physical Chemistry B,* Vol. 107, No. 31, pp. 7706–7715

Wunderlich, B. (1980). *Macromolecular Physics: Vol. 2 Crystal Nucleation, Growth, Annealing,* Academic Press, New York, USA

Zhang, J., Li, C., Duan, Y., Domb, A. J. & Ozaki, Y. (2010). Glass transition and disorder-to-order phase transition behavior of poly(l-lacticacid) revealed by infrared spectroscopy. *Vibrational Spectroscopy,* Vol. 53, No. 2, pp. 307–310

Zhang, J., Sato, H., Tsuji, H., Noda, I. & Ozaki, Y. (2005). Differences in the $CH_3 \cdots O{=}C$ interactions among poly(L-lactide), poly(L-lactide)/poly(D-lactide) stereocomplex, and poly(3-hydroxybutyrate) studied by infrared spectroscopy. *Journal of Molecular Structure.* Vol. 735–736, No. 14, pp. 249–257

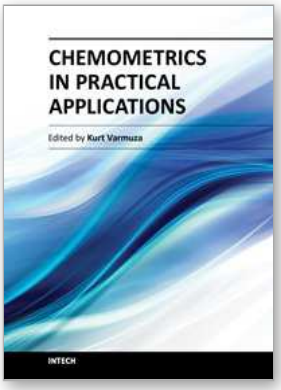

Chemometrics in Practical Applications

Edited by Dr. Kurt Varmuza

ISBN 978-953-51-0438-4
Hard cover, 326 pages
Publisher InTech
Published online 23, March, 2012
Published in print edition March, 2012

In the book "Chemometrics in practical applications", various practical applications of chemometric methods in chemistry, biochemistry and chemical technology are presented, and selected chemometric methods are described in tutorial style. The book contains 14 independent chapters and is devoted to filling the gap between textbooks on multivariate data analysis and research journals on chemometrics and chemoinformatics.

How to reference

In order to correctly reference this scholarly work, feel free to copy and paste the following:

Hideyuki Shinzawa, Masakazu Nishida, Toshiyuki Tanaka, Kenzi Suzuki and Wataru Kanematsu (2012). PARAFAC Analysis for Temperature-Dependent NMR Spectra of Poly(Lactic Acid) Nanocomposite, Chemometrics in Practical Applications, Dr. Kurt Varmuza (Ed.), ISBN: 978-953-51-0438-4, InTech, Available from: http://www.intechopen.com/books/chemometrics-in-practical-applications/parafac-analysis-for-temperature-dependent-nmr-spectra-of-poly-lactic-acid-nanocomposite

INTECH
open science | open minds

InTech Europe
University Campus STeP Ri
Slavka Krautzeka 83/A
51000 Rijeka, Croatia
Phone: +385 (51) 770 447
Fax: +385 (51) 686 166
www.intechopen.com

InTech China
Unit 405, Office Block, Hotel Equatorial Shanghai
No.65, Yan An Road (West), Shanghai, 200040, China
中国上海市延安西路65号上海国际贵都大饭店办公楼405单元
Phone: +86-21-62489820
Fax: +86-21-62489821

© 2012 The Author(s). Licensee IntechOpen. This is an open access article distributed under the terms of the Creative Commons Attribution 3.0 License, which permits unrestricted use, distribution, and reproduction in any medium, provided the original work is properly cited.